Metamaterial Based Dual-Band and Polarization Independent RF Absorber

Kadir Ozden[1], O.Mert Yucedag[2], Ahmet Ozer[2], Huseyin Bayrak[2] and Hasan Kocer[2]

[1] Defense Sciences Institute, Turkish Military Academy, Ankara, Turkey
kozden@kho.edu.tr
[2] Department of Electrical Engineering, Turkish Military Academy, Ankara, Turkey
omyucedag, aozer, hbayrak, hkocer@kho.edu.tr

Abstract

Metamaterials have great potential for the practical applications of electromagnetic wave absorption. Therefore, it is important to understand the mechanism of the metamaterial based electromagnetic wave absorbers. In this paper, the design, simulation, fabrication and measurement of a polarization independent dual-band metamaterial absorber is presented in the microwave region. The proposed metamaterial absorber shows perfect absorption peaks at 7.90 and 8.90 *GHz* which are in good agreement with the simulated results.

1. Introduction

Metamaterials are artifical structures which have novel features such as backward wave propagation, negative refractive index and phase velocity. Metamaterials with these properties are used in many practical applications such as super lenses [1], antennas [2], sensors [3] and perfect absorbers [4, 5]. The matematerial based perfect absorbers have attracted a great deal of interest in stealth technology in recent years.

Studies about metamaterials was based on a Russian physicist V. Veselago [6]. He showed negative refraction index by having negative permittivity (ε) and permeability (μ) theoretically. His studies were confirmed by Pendry *et al* nearly 30 years later [7]. After that, there has been considerable interest in metamaterials over electromagnetic (EM) spectrum. Because of their effective permittivity and permeability which can be modified to minimize both transmittance and reflectance at a resonant frequency, metamaterial based EM wave absorbers have become one of the major research areas. The first metamaterial based absorption experiments were held by Landy *et al* [4] in 2008. Initially, narrow bandwith and polarization sensitive perfect absorption was achieved. After that, most of the researches were concentrated on obtaining the polarization-independent [8], wide-angle [9], multi-band [10] and broadband absorbers [11]. Compared to the conventional millimeterwave absorbers which are physically thick and their frequency performance is limited, metamaterials are excellent candidates for electromagnetic wave absorbers, due to their ability to exhibit exotic electromagnetic and tunable effects. So, it is important to understand the pros and cons of the metamaterial based electromagnetic wave absorbers. Therefore, the geometrical parameters and thermal effect of metamaterial based absorbers are investigated [12, 13].

In this study, the design, simulation, fabrication and measurement of a polarization independent dual-band metamaterial absorber is presented. Initially , a known structure [4] is taken as a unit cell. Then, a new design is performed to get different resonances by adding new structure. Moreover, the dimensions of the metamaterial absorber is optimized to have resonances in the X-band. A polarization independent metamaterial absorber is achieved by adding $90^{\circ}C$ rotated unit cell next to the other. It is observed that the RF simulation results are in good agreement with the measurements such that perfect absorption occurs at 7.90 and 8.90 *GHz*. It should be noted that the design and analysis are carried out with CST Microwave Studio.

In section II, the design, simulation and fabrication of the metamaterial absorber are described. In addition, the simulation and measurement results are presented and discussed. To better understand the mechanism of the RF absorption, the electric and magnetic field distribution results are presented in section III. Finally, a conclusion is drawn in section IV.

2. Design, Simulation and Fabrication of the Metamaterial Absorber

The proposed metamaterial absorber consists of two metallic layers separated by a dielectric layer. The top layer consisted of two concentric square rings. The inner ring is composed of electric ring resonator (ERR) connected by the inductive wire parallel to the splits. The outer ring is made up of split ring resonator (SRR) which have two splits oriented oppositely. The second layer is metallic continuous ground plane. A schematic diagram of the unit cell can be seen in Fig. 1(a). These metallic layers are selected as conductive copper which has 17 μm thickness and its frequency independent conductivity (σ) is $5.8x10^7$ *S/m*. The dielectric material is epoxy glass cloth laminate (FR4) which has 1.6 *mm* thickness and its relative dielectric permittivity (ε_r) is 3.6 and the loss tangent ($\tan\delta$) is 0.03. The simulated metamaterial has the dimensions, in millimeters, of: L_1=7.5, L_2=6.4, L_3=3.9, *w*=0.6, *g*=0.4 and *d*=0.65.

In the simulation setup, the proposed metamaterial absorber is illuminated by a horizontally and vertically polarized plane wave in 7-10 *GHz* frequency band. The plane wave propagates along -*z* direction. Periodic type boundary conditions are applied along *x* and *y-axes* as shown in Fig. 1(b). The metamaterial absorber structure which has the dimensions of 7.5 x 7.5 *cm* (i.e., 8 unit cells along *x-axis* and *y-axis*) is fabricated using printed circuit board (PCB) technique as shown in Fig. 1(c).

In the experimental setup, as shown in Fig.2, a vector network analyzer (Net Rohde & Schwarz ZVL, 9 KHz-13.6 GHz) and a pair of double-ridged waveguide horn antennas (HF907 800MHz-18GHz) are used. The distance between the antennas is set 45 *cm* and the metamaterial absorber is located 90 *cm* away from the antennas. A pair of horn antennas serving as the source and receiver are connected to the network analyzer by using low loss flexible cables in order to measure the reflec-

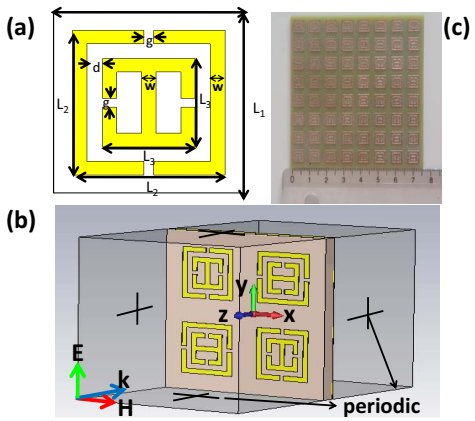

Figure 1. (a) Front view. (b) Perspective view of the simulation. (c) Photograph of the fabricated MA sample.

tion coefficient. Many pyramid absorbing materials are placed around the metamaterial absorber sample and between the antennas to eliminate the electromagnetic interference from the surrounding environment and antennas.

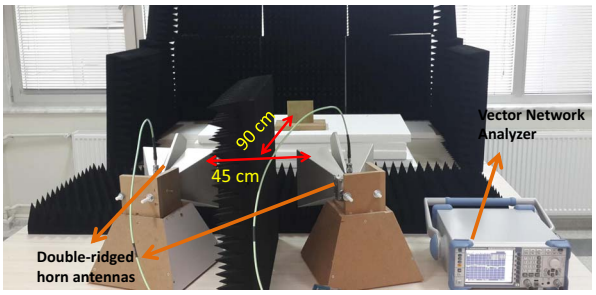

Figure 2. The experimental setup.

In order to measure standard reflection response, the completely metallic back plane of the metamaterial absorber is measured at the first phase. In the second phase, the reflection coefficient is measured by using top layer of the metamaterial absorber. The frequency dependent absorption *A(f)* of a material is related to its transmission *T(f)* and reflection *R(f)* by *A(f)*=1-*T(f)*-*R(f)*. Here, *R(f)*=$|S_{11}(f)|^2$ and *T(f)*=$|S_{21}(f)|^2$ where $S_{11}(f)$ and $S_{21}(f)$ are reflection and transmission coefficients, respectively. *T(f)* is zero due to the presence of the continuous copper ground plane. Thus, the total absorption is calculated only by the reflection. In order to achieve the maximum absorption, the reflection should be minimized.

The frequency characteristic of the absorption is presented in different polarizations, as seen in Fig. 3. It is noted that the reflection of the absorber drops to a minimum at 7.90 and 8.90 *GHz* denoting impedance matching with the free space. These results show that the RF simulation results are in good agreement with the measurements such that near-perfect and polarization independent absorption occurs at 7.90 and 8.90 *GHz*. The quality-factor can be calculated from the resonance spectra in Fig. 3 by the following equation:

$$Q = \frac{f_0}{\Delta f_{FWHM}} \tag{1}$$

Here, f_0 is the resonance frequency and Δf_{FWHM} is its half maximum width. The Q-factor from the simulation and experimental results using Eqn.1 was found to be approximately 20.28 for 7.90 *GHz* and 13.54 for 8.90 *GHz*, respectively.

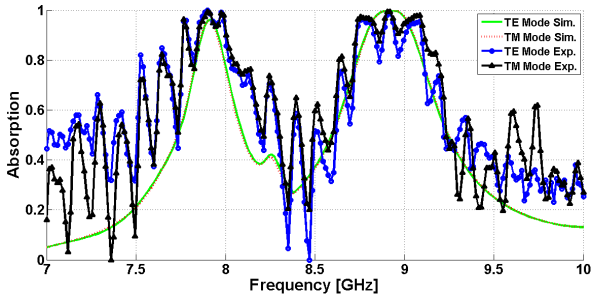

Figure 3. The simulated and measured absorption of the metamaterial absorber for TE (E field perpendicular to the ERR splits) and TM (E field parallel to the ERR splits) polarization modes.

From the retrieved equation (i.e. Eqn. (2)), both the real and imaginary part of relative wave impedance is shown in Fig. 4 at the absorptive peaks of frequency 7.90 and 8.90 *GHz* [14].

$$\hat{z} = \sqrt{\frac{(1+S_{11})^2 - S_{21}^2}{(1-S_{11})^2 - S_{21}^2}} \tag{2}$$

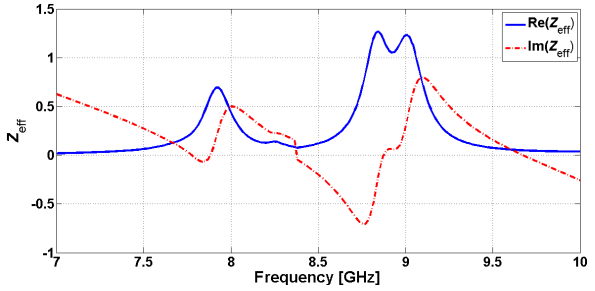

Figure 4. Real part (solid line) and imaginary part (dashed line) of relative impedance extracted from simulations.

3. Absorption Mechanism of The Metamaterial Absorber

To better understand the physical mechanism of the dual-band metamaterial absorber, electric and magnetic field distribution are plotted in Fig.5 (a, b). For horizontal and vertical polarization case, the electric field is strongly concentrated between only two of the outer and inner ring structure at 7.90 *GHz* as shown in Fig. 5(a-i, iii). However, at the 8.90 *GHz* electric field distribution is observed in ERR splits as seen in Fig. 5(a-ii,

iv). Because of this, FWHM at 8.90 *GHz* is greater than 7.90 *GHz*. It can be observed that the magnetic field distribution is concentrated strongly in the vicinity of the the inductive ring parallel to the split-wire, as seen in Fig. 5(b-i, iii). Similar to electric field distribution, the magnetic field distribution is only in two of the unit cells at 7.90 *GHz* while it is spread among all the unit cells at 8.90 *GHz* as illustrated in Fig. 5(b-ii, iv).

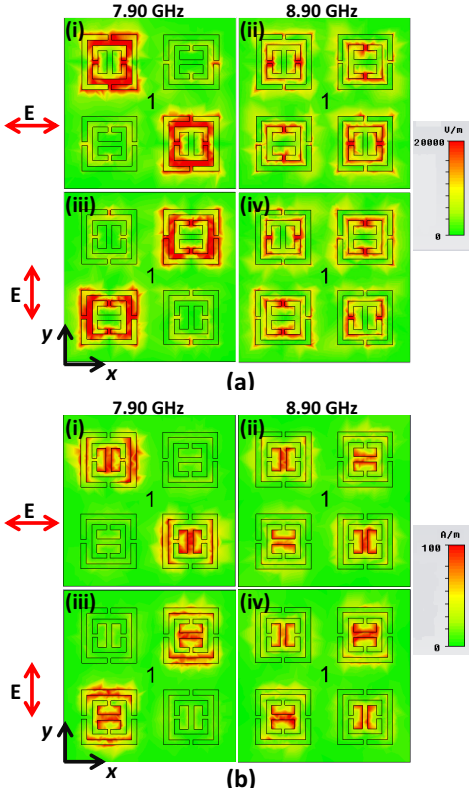

Figure 5. (a) Electric field distribution of the MA, $|E|$ field. (b) Magnetic field distribution of the MA, $|H|$ field.

4. Conclusion

In summary, a polarization independent dual-band metamaterial absorber has been successfully fabricated and measured. The proposed metamaterial presents absorption peaks at 7.90 and 8.90 *GHz* which are in good agreement with the simulated results under different polarizations of incident EM waves. To better understand the physical mechanism of the dual-band metamaterial absorber, electric and magnetic field distribution are plotted. By broadening bandwidth, metamaterials have great potential of cloaking and stealth technology applications. With geometrical scalability, the broadband metamaterial absorber can be achieved by overlapping the absorption peaks of the unit cells when their peaks are closed to each other.

Depending on these results, it is possible to say that, metamaterials have great promise for future applications such as frequency selective surfaces, EM wave spatial filter, etc.

5. Acknowledgement

This research was supported by Ankara University and the 3rd AFSM. The authors are thankful to Associate Professor A.E.YILDIZ and Research Assistant S.CAN for their contributions in preparing the experimental setup and 3rd AFSM to for their cooperation to fabricate the samples. Note that, K.Ozden is supported by The Scientific and Technological Research Council of Turkey (TUBITAK) through a postgraduate scholarship program.

6. References

[1] N. Fang, H. Lee, C. Sun and X. Zhang, "Subdiffraction-limited optical imaging with a silver superlens", *Science*, vol. 308, no. 5721, pp. 534-537, 2005.

[2] L.M. Si, and X. Lv, "CPW-FED multi-band omni-directional planar microstrip antenna using composite metamaterial resonators for wireless communications", *Prog. Electromag. Res.*, vol. 83, pp. 133-146, 2008.

[3] N. Liu, M. Mesch, T. Weiss, M. Hentschel and H. Giessen, "Infrared perfect absorber and its application as plasmonic sensor", *Nano Lett.*, vol. 10, no. 7, pp. 2342-2348, 2010.

[4] I.N. Landy, S. Sajuyigbe, J.J. Mock, D.R. Smith and W.J. Padilla, "Perfect metamaterial absorber", *Phys. Rev. Lett.*, vol. 100, no. 20, pp. 207402, 2008.

[5] L. Li, Y. Yang and C. H. Liang, "A wideangle polarization-insensitive ultra-thin metamaterial absorber with three resonant modes", *J. Appl. Phys.*, vol. 110, no. 6, pp. 063702, 2011.

[6] V.G. Veselago, "The electrodynamics of substances with simultaneously negative values of ε and μ," *Sov. Phys.Uspekhi*, Vol. 10, no. 4, pp. 509-514, 1968.

[7] J.B. Pendry, A.J. Holden, D.J. Robbins and W.J. Stewart, "Magnetism from conductors and enhanced nonlinear phenomena", *IEEE Trans.Microw.Theory Tech*, vol. 47, no. 11, pp. 2075-2084, 1999.

[8] B.,Zhu, Z. Wang, C. Huang, Y. Feng, J. Zhao and T. Jiang, "Polarization insensitive metamaterial absorber with wide incident angle," *Prog. Electromag. Res.*, vol. 101, pp. 231-239, 2010.

[9] X. J.He, Y. Wang, T.L. Gui and Q. Wu, "Dual-band terahertz metamaterial absorber with polarization insensitivity and wide angle", *Prog. Electromag. Res.*, vol. 115, pp. 381-397, 2011.

[10] B.R. Bian, S.B. Liu, S.Y. Wang, X.K. Kong, H.F. Zhang, B. Ma and H. Yang, "Novel triple-band polarization-insensitive wide-angle ultra-thin microwave metamaterial absorber", *J. Appl.Phys.*, vol. 114, no. 19, pp. 194511, 2013.

[11] B.Y. Wang, S.B. Liu, B.R. Bian, Z.W. Mao, X.C. Liu, B. Ma and L. Chen, "A novel ultrathin and broadband microwave metamaterial absorber", *J. Appl.Phys.*, vol. 116, no. 9, pp. 094504, 2014.

[12] K. Ozden, O.M. Yucedag and H. Kocer, "Geometrical parameter investigation of metamaterial absorber for space based remote sensing applications.", *Recent Advances in Space Technologies.*, Istanbul, Turkey, 2015.

[13] K. Ozden, O.M. Yucedag, A. Ozer, H. Bayrak, H. Isik and H. Kocer, "Thermal imaging of RF induced heat loss in a microwave metamaterial absorber.", *Progress In Electromagnetic Research Symposium*, Prague, Czech Republic, 2015.

[14] Z. Szabo, G.H. Park, R. Hedge and E.P. Li, “A unique extraction of metamaterial parameters based on Kramers - Kronig relationship”, *IEEE Trans. Microwave Theory Tech.*, vol. 58, no. 10, pp. 2646-2653, 2010.